Basic Bifurcation Phenomena

World of Bifurcation (WOB): Tutorial 2

Rüdiger Seydel[1]

March 2026

Models describing our nonlinear phenomena are defined by the language of mathematics. The equations representing the models can be ordinary differential equations (ODEs), or partial differential equations (PDEs). Moreover, some problems are described by "algebraic" equations, or by integral equations, or by some mixture. In addition to differential equations there may be boundary conditions or initial conditions. Faced with the great variety of possible combinations and formats we basically restrict ourselves to the ODE situation. Many of the ideas and methods can be applied in similar ways to other equations.

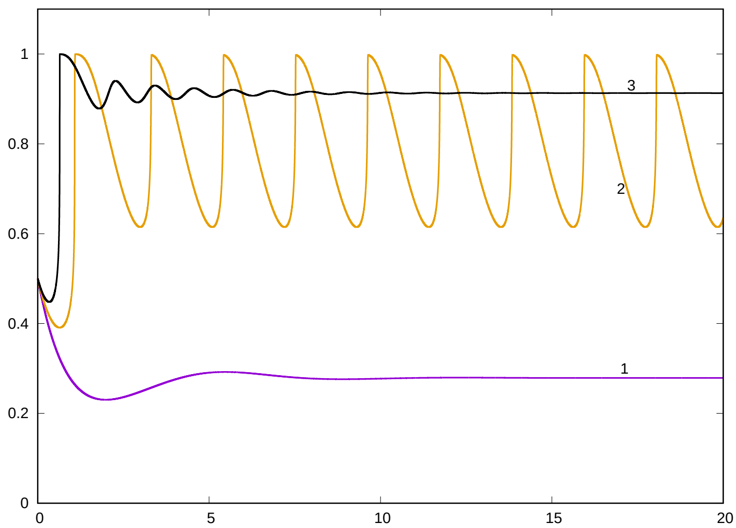

Figure 2.1: Computer experiment on Eq.(2.1). Horizontal axis: time t for $0 \le t \le 20$, vertical axis: solutions $y_1(t)$; behavior of y_1 for the three parameter values $\lambda_1 = 0.125$ (violet, 1), $\lambda_2 = 0.2$ (orange, 2), $\lambda_3 = 0.26$ (black, 3), initial values $y_1(0) = y_2(0) = 0.5$

2.1 A computer experiment

For time $t \ge 0$ we define $y_1(t)$ and $y_2(t)$ to be functions that solve the system of two ODEs

$$\begin{aligned} \dot{y}_1 &= -y_1 + \lambda(1-y_1)\exp(y_2) \\ \dot{y}_2 &= -y_2 + 16.2\,\lambda\,(1-y_1)\exp(y_2) - 3y_2 \end{aligned} \tag{2.1}$$

and satisfy the initial values

$$y_1(0) = 0.5\,, \quad y_2(0) = 0.5\,;$$

for the background of a continuous stirred tank reactor see WOBexd2[2]. Functions y_1 and y_2 are *state variables*, they depend on each other according to Eq.(2.1). The symbol λ stands for

[1]Universität zu Köln, Mathematisches Institut, e-mail: rseydel@uni-koeln.de

[2]References to applications at the end of this Tutorial 2; WOB refers to www.bifurcation.de

a parameter that may take values in a range, say, between 0.125 and 0.26. The parameter λ is independent of the state variables and assumed constant. But λ might change due to some outer control, thereby influencing the state variables. This will be our concern in the following.

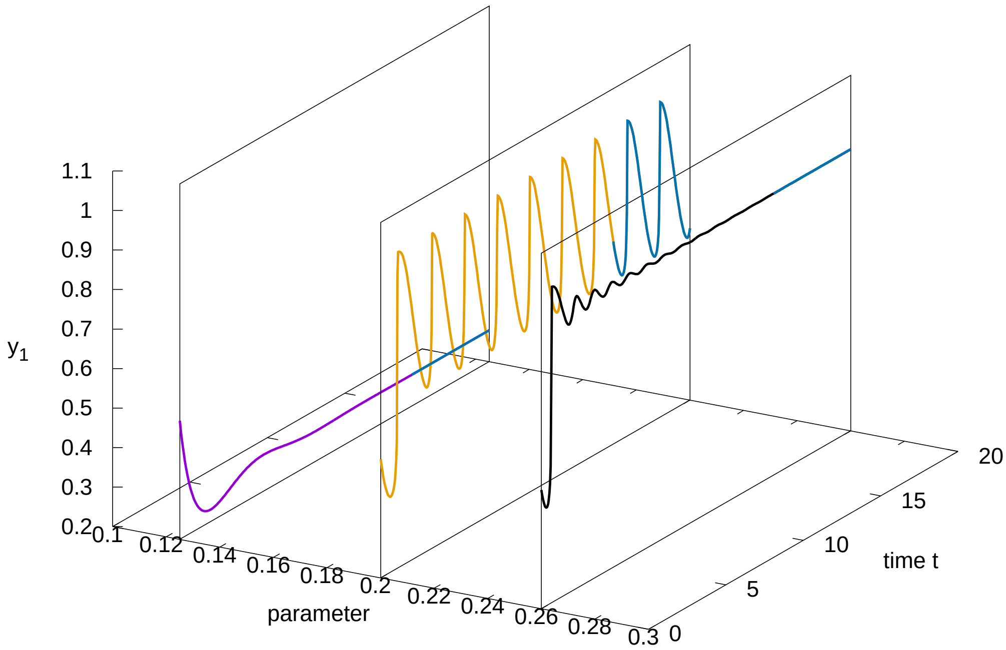

Figure 2.2: Computer experiment as in Figure 2.1, but now the plots for λ_1, λ_2, λ_3 are separated into three planes. The trajectories are attracted by their respective *attractor*, for $15 \leq t \leq 20$ emphasized by blue color. — What happens for other values of the parameter?

Take any code for integrating ODE initial-value problems, and integrate the equations, say, for the time interval $0 \leq t \leq 20$. For the first series of experiments we take constant values of λ for each integration, and change λ from one integration to the next. In Figure 2.1 we observe the results for three selected values of λ, namely $\lambda_1 = 0.125$, $\lambda_2 = 0.2$, and $\lambda_3 = 0.26$. For example, take $\lambda_1 = 0.125$ as a first experiment. We observe (violet curve) that after a *transient phase* of, say, $0 \leq t \leq 10$, the trajectory $y_1(t)$ becomes *stationary* — that is, the trajectory is attracted by a state with a constant value. For the second choice $\lambda_2 = 0.2$ the situation ist quite different: After a transient phase the trajectory becomes periodic with large oscillations (orange curve in Figure 2.1). The stationary state, and the periodic state respectively attract neighboring trajectories. Both attracting states are regular in shape (stationary, periodic). Finally, for the third experiment with parameter $\lambda_3 = 0.26$, the attractor is again stationary, but now on a higher level. This series of experiments has shown that the level and the quality of solutions *vary with the parameter*.

This treatment of the parameter λ as being constant but variable is called *quasistationary* variation. We have seen attractors for the three distinct λ-values λ_1, λ_2, λ_3. What happens inbetween for other values of the parameter (Figure 2.2)? Attractors might disappear, or drift in the phase space. There must be some transition between the attractors.

To come closer to an answer, we perform a second type of experiment, and let the parameter drift slowly in a nonstationary way, $\dot{\lambda} \neq 0$. In order to move with the parameter through a range that matches the first set of experiments, we choose artificially the additional differential equation

$$\dot{\lambda} = 0.001, \quad \lambda(0) = 0.1$$

We may denote $y_3 := \lambda$ and integrate a coupled system of three ODEs for $0 \leq t \leq 200$. The result is seen in Figure 2.3. Because of the linear variation of λ, the horizontal axis can be exchanged by an equivalent λ-axis extending from $\lambda = 0.1$ to $\lambda = 0.3$, which would indicate the current value of the parameter. Observing the result of Figure 2.3, we come closer to an

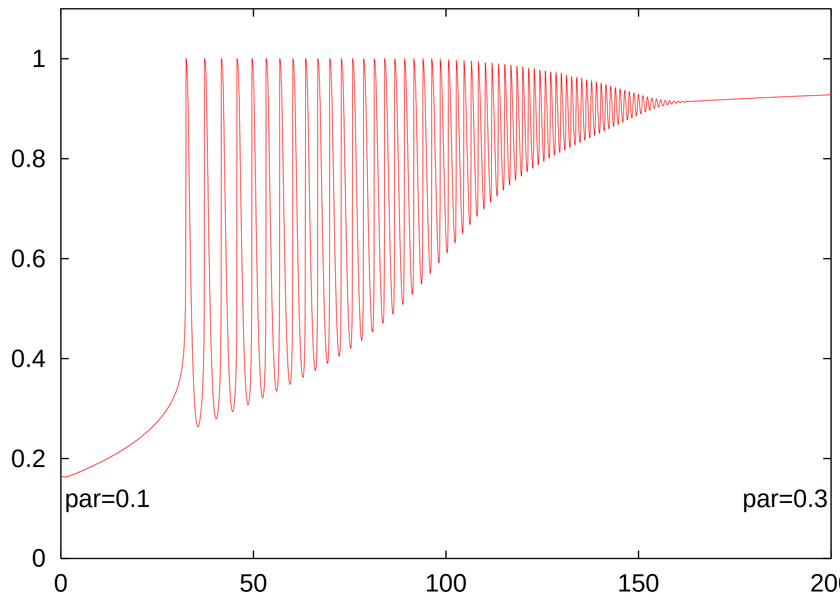

Figure 2.3: Computer experiment, axes as before in Figure 2.1. Now the parameter λ does not take constant values but varies linearly from 0.1 (for $t = 0$) to 0.3 (for $t = 200$). Apparently, several different attractors are passed, from stationary low level to strong oscillations to stationary higher level.

explanation of our quasistationary treatment reported above. There appears to be a sudden *jump* from a more or less stationary state to a strongly oscillating state at $t \approx 40$ ($\lambda \approx 0.14$). For further increasing t (or λ) the amplitude of the oscillation diminishes and dies out for $t \approx 150$ ($\lambda \approx 0.25$). Since λ is not constant, the experiment reported in Figure 2.3 does not settle into a purely stationary or purely periodic state (blue in Figure 2.2). Apparently, for drifting parameters the location of the attractor varies continuously, and trajectories follow. Summarizing this experiment we note that for $\lambda \approx 0.14$ and $\lambda \approx 0.25$ a *threshold* of the parameter is passed. Later we shall explain such thresholds and the mechanism of switching attractors as *bifurcations*.

2.2 A model problem

Often biological, physical, technical ... problems are modelled by a first-order system of ODEs

$$\dot{\mathbf{y}} = \mathbf{f}(\mathbf{y}, \lambda) \tag{2.2}$$

where $\mathbf{y}(t)$ is a vector function with n components $y_i(t)$, $i = 1, \ldots, n$. In Eq.(2.1) $n = 2$. The overdot indicates differentiation with respect to time t, and $\mathbf{f}$ is the *right-hand side* defining the dynamical law. The state $\mathbf{y}$ that solves Eq.(2.2) depends on the real parameter $\lambda \in \mathbb{R}$. *Periodic solutions* of the autonomous system Eq.(2.2) satisfy $\mathbf{y}(t + T) = \mathbf{y}(t)$ for all t and a minimum period $T > 0$. We call such solutions also periodic orbits. *Stationary solutions* $\mathbf{y}^{\mathrm{s}}$ of Eq.(2.2) solve

$$\mathbf{f}(\mathbf{y}, \lambda) = \mathbf{0}\,. \tag{2.3}$$

A system of equations like Eq.(2.3) also describes applications without the background of a dynamical system Eq.(2.2).

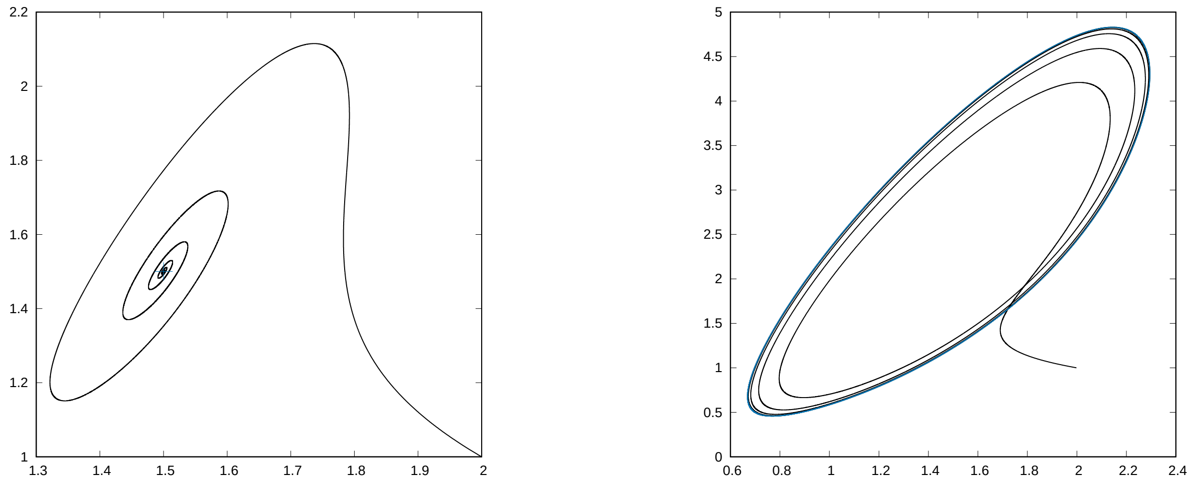

Figure 2.4: Equation (2.4); (y_1, y_2)-phase diagrams (projections of the three-dimensional phase space to the (y_1, y_2)-plane) with two trajectories. Parameter $\lambda = 1$ (left, convergence to an equilibrium), and $\lambda = 1.5$ (right, convergence to a periodic orbit), initial vector of the trajectories is (2, 1, 1), time $0 \leq t \leq 40$. Attractors are indicated in blue.

2.3 An example from chemistry

As an example consider a chemical reaction with autocatalytic step (WOBexd6)

$$\begin{aligned} \dot{y}_1 &= 3 - y_1 - \lambda y_1 y_3 \,, \\ \dot{y}_2 &= y_1 - y_2 y_3 \,, \\ \dot{y}_3 &= y_2 y_3 - \lambda y_1 y_3 \,. \end{aligned} \tag{2.4}$$

Equation (2.4) is of the format of (2.2), with $n = 3$. In Figure 2.4 we show in phase-plot projections $(y_1(t), y_2(t))$ two trajectories converging towards attractors. Since the trajectories $\mathbf{y}(t)$ of Eq.(2.4) move in the three-dimensional phase space $\mathbb{R}^3$ we have projected the curves in space to a (y_1, y_2)-plane for easy graphical demonstration. Starting from $\mathbf{y}(0) = (2, 1, 1)$ we show the transient initial phase where the trajectories approach the "next" attractor. Figure 2.4 (for $\lambda = 1$, left figure) depicts a situation with a stable stationary point (spiral), and the right-hand figure ($\lambda = 1.5$) shows a projection of the dynamics of an attracting periodic orbit. Note that the trajectories do not intersect in the reality of the phase space $\mathbb{R}^3$. The attractors are *stable*—that is, the impact of small perturbations decays to zero.

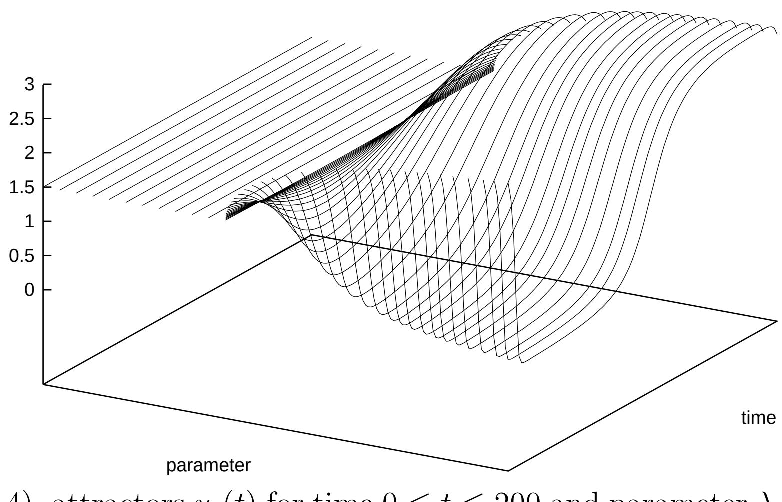

Figure 2.5: Eq.(2.4), attractors $y_1(t)$ for time $0 \leq t \leq 200$ and parameter λ with several values from 0.1 to 0.3

2.4 Hopf bifurcation

As noted above, solutions $\mathbf{y}$ depend on time t, and on the parameter λ. Both dependencies are indicated in Figure 2.5, where we show solution profiles $y_1(t;\lambda)$ for several discrete values of the parameter λ out of the interval $0.2 \le \lambda \le 3$. These slices correspond to the slices in the example of Figure 2.2. In Figure 2.5 the slices are narrow so that we may see a hint on what is going on. We observe two different regimes, separated by a parameter value of about $\lambda_0 \approx 1.3$ [more exactly[3] $\lambda_0 = 1.302$]. For small values of the parameter, the solution profiles in Figure 2.5 reflect stable stationary states. And for parameter values larger than λ_0 the solution profiles represent stable periodic solutions. Their amplitude grows with growing parameter, emerging at λ_0 with amplitude 0. At this parameter value, periodic orbits are born. This phenomenon of a birth of periodic orbits out of stationary solutions is called *Hopf bifurcation*.

The period varies too; the initial period for λ_0 is $T_0 = 6.036$. Figure 2.5 depicts the values of $y_1(t)$ for one period; the periods are scaled to unity. The two other components y_2, and y_3 vary similarly. Figure 2.5 depicts the asymptotic situation with attracting stationary and periodic states; transient initial phases are not shown. The stability of the solutions is illustrated by the phase diagrams of Figure 2.4.

Hopf bifurcation serves as an organizing center, separating different regimes of attracting states. This prominent role of Hopf bifurcation deserves a proper graphical illustration. We call it *bifurcation diagram*. That of Eq.(2.4) is shown in Figure 2.6. The choice of the vertical axis is not unique. Here we have chosen y_1 at some reasonable value of t. Since attractors (as well their counterparts *repellors*) play an important role in organizing the dynamical behavior of trajectories, bifurcaction diagrams illustrate the *skeleton of the dynamical behavior*.

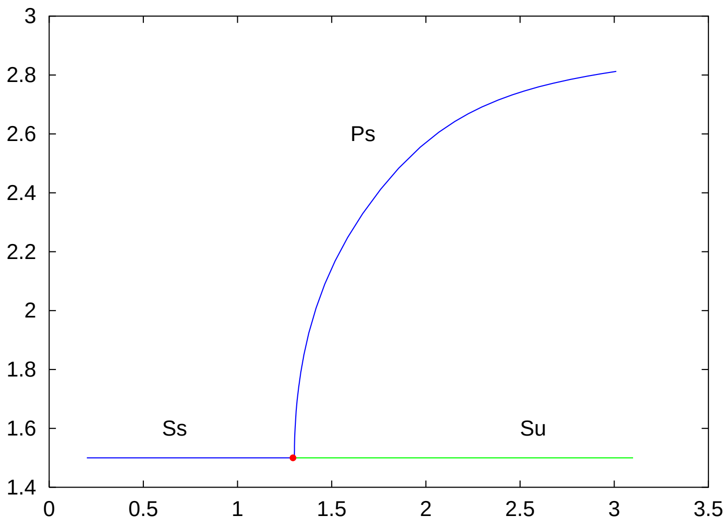

Figure 2.6: Equation (2.4); bifurcation diagram of underlying attractors, y_1 (at some time t) is plotted over parameter λ. Ps stands for periodic stable, Su for stationary unstable, Ss for stationary stable; blue indicates stability and green indicates instability. The red dot marks the bifurcation point.

Looking back to Eq.(2.1) with Figures 2.1 and 2.2, we had left gaps between the discrete parameter values λ_1, λ_2, λ_3. The explanation of the disclosed phenomena is again Hopf bifurcation, see Figure 2.7. There are stationary solutions for a wide range of λ-values, but between the two Hopf bifurcation points all are unstable. At the right-hand bifurcation with critical value $\lambda_0^{\mathrm{b}} = 0.2465$, there are stable periodic orbits for a range of parameter values with $\lambda < \lambda_0^{\mathrm{b}}$; these orbits start at λ_0^{b} with zero amplitude. We speak of a *soft generation* of limit cycles.

The situation is quite different at the left-hand Hopf bifurcation with $\lambda_0^{\mathrm{a}} = 0.1300$. Here neighboring periodic orbits exist for a narrow range of parameter values with $\lambda < \lambda_0^{\mathrm{a}}$, but they

[3] We round to 4 decimal digits

are unstable. Therefore trajectories for $\lambda > \lambda_0^{\mathrm{a}}$ immediately jump to a periodic stable orbit, which is quite distant. At the Hopf point λ_0^{a} there is no continuous transition from unstable stationary to stable periodic. In this situation we speak of a *hard generation* of limit cycles. This explains the sudden jump-wise onset of periodic orbits demonstated in Figures 2.1 and 2.2.

Now the dynamic behavior of the trajectory shown in Figure 2.3 is clarified. The drifting parameter λ passes both Hopf values λ_0^{a} and λ_0^{b}. The skeleton shown in Figure 2.7 underlying this dynamical system is the key to understand the situation.[4] In Figure 4 of Tutorial 1, Figure 2.3 is covered by the bifurcation diagram, which strikingly highlights the role of our skeleton.

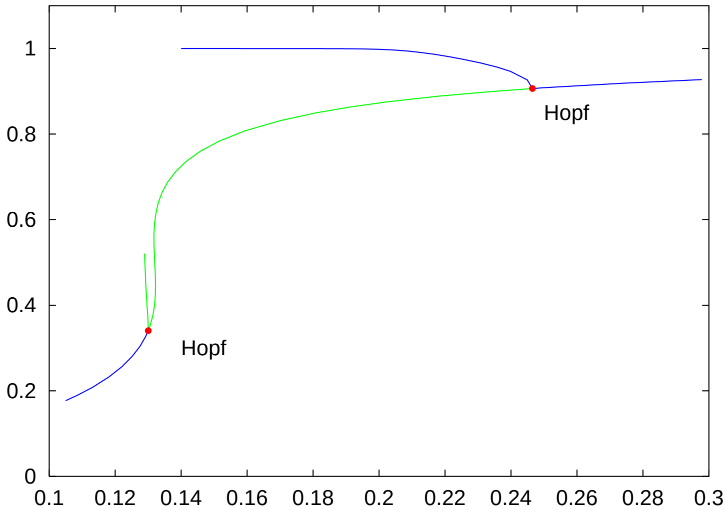

Figure 2.7: Example of Eq.(2.1): bifurcation diagram, representing the skeleton of dynamical behavior; colors as in Figure 2.6: blue for stable and green for unstable.

2.5 Branches

As illustrated by the above examples and computer experiments, solutions in general vary when the parameter is changed. Figures 2.1 and 2.2 have shown solutions for a discrete selection of λ values. We could have chosen any intermediate value of λ and would have obtained solutions between those depicted. There is a *continuum* of solutions parameterized by λ. The slices in Figure 2.5 extend to a continuous surface. We call a smooth continuum of solutions a *branch*. Mostly this refers to attractors and repellors. Accordingly, the bifurcation diagrams of Figures 2.6 and 2.7 represent branches.

The implicit function theorem (see any textbook of analysis) specifies sufficient criteria guaranteeing that a branch can be parameterized by λ. For a specific stationary solution $(\mathbf{y}^{\lambda_1}, \lambda_1)$ of Eq.(2.2) the criterion basically requires nonsingularity of the Jacobian matrix $\mathbf{f}_{\mathbf{y}}(\mathbf{y}^{\lambda_1}, \lambda_1)$ of the first-order partial derivatives. Then there is an interval around λ_1 such that for all λ in that interval Eq.(2.2) has a solution $\mathbf{y}^{\lambda}$ close to $\mathbf{y}^{\lambda_1}$.

[4]It may be helpful to enter notations Ps, Su, Ss into Figure 2.7, and follow the path of λ of Figure 2.3.

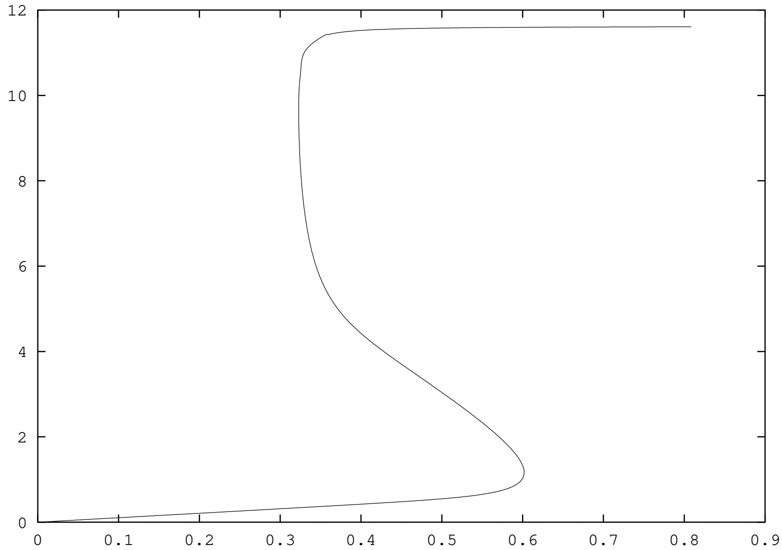

Figure 2.8: Trigger, Eq.(2.5), output voltage y_6 versus input voltage λ.

2.6 An example from electrical engineering

A trigger circuit (WOBexa2) is defined by

$$\begin{aligned}
f_1 &= (y_1 - y_3)/10000 + (y_1 - y_2)/39 + (y_1 + \lambda)/51 = 0, \\
f_2 &= (y_2 - y_6)/10 + I(y_2) + (y_2 - y_1)/39 = 0\,, \\
f_3 &= (y_3 - y_1)/10000 + (y_3 - y_4)/25.5 = 0\,, \\
f_4 &= (y_4 - y_3)/25.5 + y_4/0.62 + y_4 - y_5 = 0\,, \\
f_5 &= (y_5 - y_6)/13 + y_5 - y_4 + I(y_5) = 0\,, \\
f_6 &= (y_6 - y_2)/10 - [U_\mathrm{A}(y_3 - y_1) - y_6]/0.201 + (y_6 - y_5)/13 = 0\,;
\end{aligned} \tag{2.5}$$

where

$$U_\mathrm{A}(U) := 7.65 \arctan(1962\,U), \quad I(U) := 5.6 \cdot 10^{-8}(\mathrm{e}^{25U} - 1)\,.$$

This problem is of the form of Eq.(2.3), $\mathbf{f}(\mathbf{y}, \lambda) = \mathbf{0}$, with $n = 6$. The variables y_i are voltages. The input voltage is λ, the output voltage is y_6. Solving Eq.(2.5) yields the *hysteresis*-type response diagram in Figure 2.8. The branch of solutions is a (one-dimensional) curve in the seven-dimensional $(\mathbf{y}, \lambda)$-space. In Figure 2.8 the curve is a projection to the (y_6, λ)-plane.

In this example of a trigger the essential theme is *bistability*. Here the bistable situation is characterized by two bounding critical solutions where the branch can not be parameterized by λ; the tangent to the branch in these points is "vertical" (i.e., perpendicular to the λ-axis). These two *turning points* of Eq.(2.5) have the threshold values $\lambda_0 = 0.6019$, and $\lambda_0 = 0.3229$. When moving along the lower branch in Figure 2.8 towards the turning point, the electrical circuit experiences a well-designed jump to the upper branch, viz. to the higher voltage. On the other hand, when on the upper branch the input voltage λ is diminished, there is again a jump, now to the lower level. Obviously the turning points are thresholds where jumps to the other stable level take place. At these critical solutions the Jacobian matrix $\mathbf{f}_\mathbf{y}$ is singular. But note that the curve can be parameterized by y_6. A turning point is also called *fold bifurcation*, or *saddle node*.

Fold bifurcations / turning points are frequently occurring in applications. For a boundary value problem (not of the type of Eq.(2.2)) see the Duffing oscillator WOBexb3, or the catalytic reaction WOBexb1, or the electric power system WOBexd15.

Diagrams like Figure 2.8 depicting a scalar representative of $\mathbf{y}$ versus the parameter λ are also called *branching diagram*[5], or *response diagram*, we have seen them in Figures 2.6 and 2.7.

[5] We use "bifurcation" and "branching" as synonyms.

2.7 General bifurcation

We already have discussed the phenomenon of Hopf bifurcation, the transition between stationary and periodic orbits. Hopf bifurcation is a special case of bifurcation; there are more types. Loosely speaking, a *bifurcation with respect to* λ is a specific solution at λ_0 where there is no neighborhood around λ_0 such that in this neighborhood the branch can be uniquely extended. In short, at a bifurcation something "happens." Qualitative changes are tied to bifurcations. The two turning points in the trigger problem (see Figure 2.8) are examples of bifurcation points.

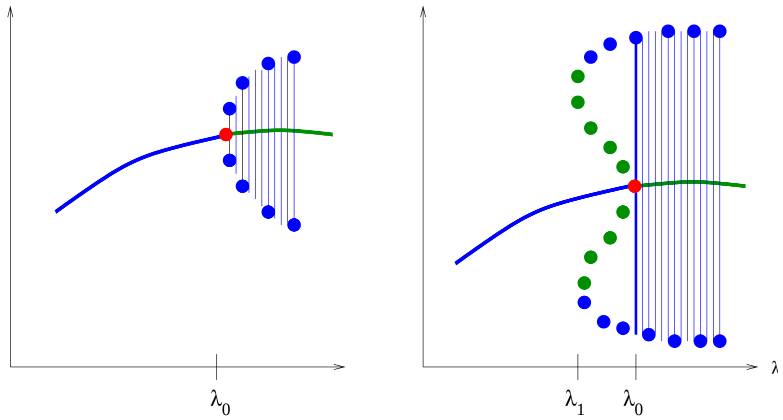

Figure 2.9: Hopf scenarios, schematical. Hopf points at respective values λ_0 are marked with red dots, stable orbits in blue symbolized by blue vertical lines ending at fat dots, instable orbits in green. left: soft loss of stability, smooth transition. right: hard loss of stability. bistability for $\lambda_1 < \lambda < \lambda_0$ of a stationary and a periodic solution

At a Hopf bifurcation, the branch of stationary solutions does not bifurcate; the Jacobian matrix $\mathbf{f_y}(\mathbf{y}_0, \lambda_0)$ is nonsingular. In Figure 2.6, for example, the branch of stationary solutions extends beyond λ_0, but they are unstable for $\lambda > \lambda_0$. The Jacobian matrix at a Hopf bifurcation has a pair of purely imaginary eigenvalues $\pm i\beta$. Here a branch of periodic orbits is born. In Figure 2.9, left sketch, for $\lambda > \lambda_0$, $\lambda \to \lambda_0$ the periodic solutions merge into the stationary branch without jump, the amplitude vanishes. The bifurcation is vertical, and the amplitude locally behaves like $\sqrt{|\lambda - \lambda_0|}$. This is seen in Figure 2.5, just concentrate on the y_1-values belonging to the minimum t-value. The vertical axes in Figures 2.6, 2.7, 2.9 depict a scalar measure of the solutions, such as

$$[\mathbf{y}] = y_1(t^*) \quad \text{where } \dot{y}_1(t^*) = 0\,.$$

That is, $[\mathbf{y}]$ depicts a relative maximum, or minimum of y_1. With this illustration, periodic oscillations can be visualized as in Figure 2.9.

In the right-hand sketch of Figure 2.9 we illustrate a situation where locally no stable state exists on one side of λ_0 (here for $\lambda > \lambda_0$). Globally, this local scenario often extends to a different situation, as drawn in the figure: The branch of unstable periodic orbits bends back, gaining stability at a turning point for λ_1. Consequently, when we increase λ beyond the critical Hopf parameter value λ_0 a jump occurs. For $\lambda > \lambda_0$, there are no neighboring small-amplitude periodic solutions, and the dynamics is immediately attracted by a large-amplitude oscillation. This large jump is the *hard loss* of stability. Figure 2.9 shows a bistable situation for $\lambda_1 < \lambda < \lambda_0$. This is the situation of Figure 2.7, left bifurcation. In fact, in a narrow λ-range the branch of unstable periodic orbits bends back, and gains stability at a turning point (not shown in Figure 2.7). — Note that the described scenarios may also happen for *de*creasing λ.

Other examples of hard loss of stability are the bogie model (WOBexd10), the nerve model WOBexd14, and the power system WOBexd15. Examples of a soft loss of stability are the Brusselator (WOBexd1), and the reaction of Eq.(2.4). In any arbitrary example of the type of Eq.(2.2) one must expect the occurrence of a fold bifurcation (turning point), or of a Hopf bifurcation.

There are other bifurcations which are less likely to be found in a general equation. But many equations involve some symmetry, for example,

$$\mathbf{f}(-\mathbf{y}, \lambda) = -\mathbf{f}(\mathbf{y}, \lambda)\,.$$

Often the symmetry in the equations reflects the common situation that a model consists of two or more identical parts that are coupled. When two identical subsystems are suitably coupled, one can exchange their states by a simple reflection. The related symmetry is the Z_2-symmetry. For equations with a Z_2-symmetry, *pitchfork bifurcation* is common too:

For a Z_2-pitchfork bifurcation, the emanating branch consists of solutions that lose their symmetry. This phenomenon is called *symmetry breaking*. Schematically, the situation is shown in Figure 2.10. The related bifurcation diagrams resemble those of Figure 2.9 of the Hopf scenario. The two asymmetric half-branches can be identified because they are transformed into each other by the underlying reflection that describes the exchange of the states of the subsystem.

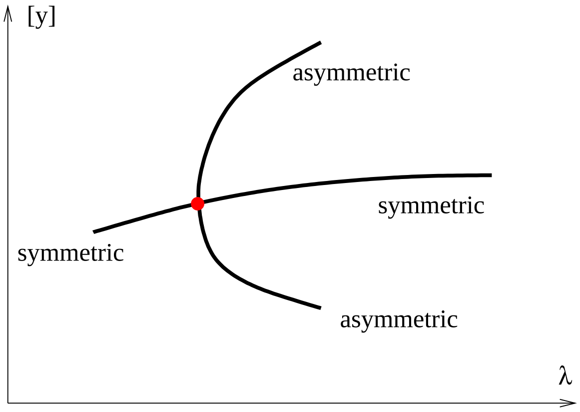

Figure 2.10: Z_2-Pitchfork Scenario

Examples of such pitchfork bifurcations are the Brusselator reaction WOBexa1, the flipflop WOBexa11, WOBexd1, the superconductivity WOBexb2, and the Duffing oscillator WOBexb3.

2.8 Period doubling and chaos

So far we mainly have studied solutions of Eq.(2.2) being regular in the sense *stationary*, or *periodic*. In addition, the deterministic system Eq.(2.2) allows for aperiodic solutions that have been named *chaotic*. There are several ways how to explain the onset of chaos. One of the most suggestive scenarios of chaos is tied to *period doubling*.

Local stability of a periodic orbit $\mathbf{y}$ is determined by the eigenvalues of the monodromy matrix $\mathbf{M} := \Phi(T)$ where $\Phi(t)$ is the matrix function that solves the linear matrix initial-value problem

$$\dot{\Phi} = \mathbf{f_y}(\mathbf{y}, \lambda)\Phi, \quad \Phi(0) = \mathbf{I}\,, \tag{2.6}$$

$\mathbf{I}$ denotes the identity matrix. These eigenvalues of $\mathbf{M}$ are called *multipliers*. One of the n multipliers is always unity, $\mu_n = 1$. The other $n-1$ multipliers $\mu_1, \ldots, \mu_{n-1}$ are monitored to examine whether they are inside the unit circle ($|\mu| < 1$), or outside. The periodic orbit is locally stable in the case when all $n-1$ multipliers are inside the unit circle. Also the multipliers depend on the parameter, $\mu = \mu(\lambda)$. Varying λ can result in one or more multipliers crossing the unit circle. Assume this happens for λ_0 — that is, $|\mu_j(\lambda_0)| = 1$ for some j. Then the solution

$\mathbf{y}$ corresponding to λ_0 is a bifurcation. Different types of bifurcation occur depending on *where* $\mu_j(\lambda)$ crosses the unit circle. The so-called period doubling happens in the case $\mu_j(\lambda_0) = -1$.

Dynamically, the period doubling bifurcation (or *flip bifurcation*) is the following scenario: Assume a branch of periodic solutions parameterized by λ with stable orbits on one side of λ_0 (say, $\lambda < \lambda_0$) and a multiplier crossing the unit circle with $\mu(\lambda_0) = -1$. Then, locally near λ_0, there are periodic orbits with the double period. These double-periodic orbits form a new branch that emerges at λ_0. Note that the periods vary with λ, and the factor 2 of period doubling holds only asymptotically for $\lambda \to \lambda_0$. The situation typically is as in Figure 2.11, for $\lambda = \lambda_{\mathrm{PD1}}$.

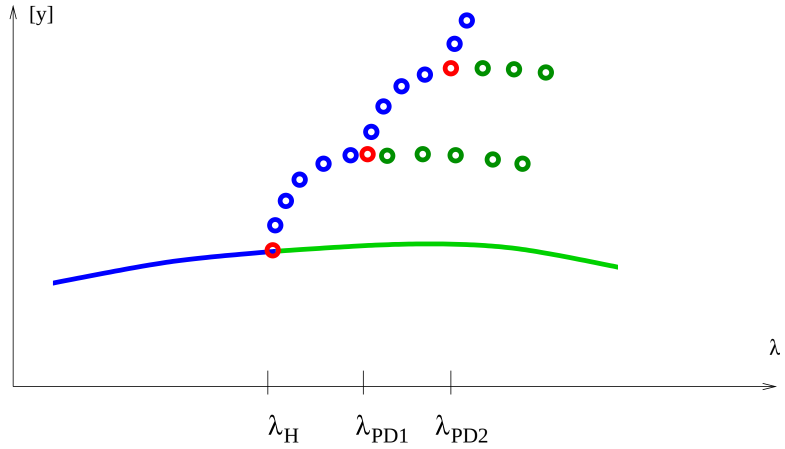

Figure 2.11: Cascade of period doublings, schematically, starting from Hopf bifurcation at λ_{H}. Colors as in Figure 2.9

The "new" branch with the "double" period can experience a period doubling, too (in Figure 2.11, for λ_{PD2}). There are many important applications where an infinite chain of such period doublings occurs. We denote them λ_{01}, λ_{02}, λ_{03}, ... Often the stability is exchanged to the branches of the double period. After some period doublings the period has become so large that the orbit looks irregular. As has been shown, the bifurcation values $\lambda_{0\nu}$ satisfy a universal scaling law,

$$\lim_{\nu\to\infty} \frac{\lambda_{\nu+1} - \lambda_\nu}{\lambda_\nu - \lambda_{\nu-1}} = 0.214169\ldots \tag{2.7}$$

This scaling law, named after Feigenbaum, has a remarkable consequence: There is an accumulation point λ_∞ of the sequence of period doubling bifurcations. Passing λ_∞ means that the "period" has reached infinity. The resulting solution is fully aperiodic, and is "chaotic." In this scenario the irregularity of a chaotic solution can be explained by the infinite number of unstable periodic orbits (UPOs) that are "left behind" at the infinite sequence of period doublings. Imagine the $\mathbf{y}$-state space is packed with UPOs, all repelling any trajectory that searches a path through that area. This state of continuously being pushed by UPOs may explain the sensitive dependence on initial conditions that is a characterisitic criterion of chaos.

2.9 An example: isothermal reaction

An isothermal reaction (see also WOBexd13) is modelled by

$$\begin{aligned} \dot{y}_1 &= y_1(30 - 0.25y_1 - y_2 - y_3) + 0.001y_2^2 + 0.1\,, \\ \dot{y}_2 &= y_2(y_1 - 0.001y_2 - \lambda) + 0.1\,, \\ \dot{y}_3 &= y_3(16.5 - y_1 - 0.5y_3) + 0.1\ . \end{aligned} \tag{2.8}$$

There is a Hopf bifurcation at $\lambda_0 = 12.14$, and a sequence of period doubling bifurcations,

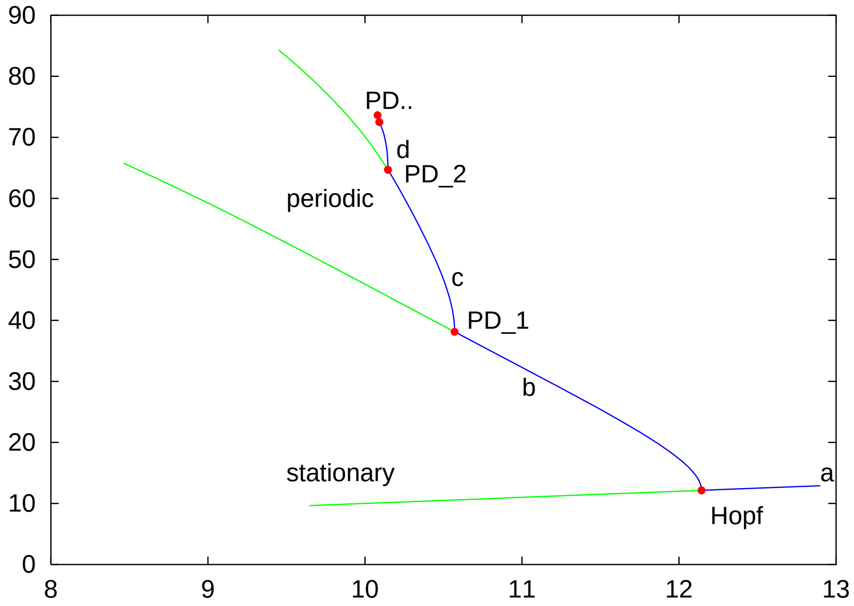

Figure 2.12: Eq.(2.8), bifurcation diagram $y_1(0)$ versus λ. The chain of branches with stable solutions a, b, c, d is a transition from stationary (a) to simple periodic (b) to double periodic (c) to fourfold periodic (d).

compare the bifurcation diagram Figure 2.12. Critical parameter values $\lambda_{0\nu}$ or λ_ν of period doubling are

$$\begin{aligned} \lambda_1 &= 10.57 \\ \lambda_2 &= 10.15 \\ \lambda_3 &= 10.09 \\ \lambda_4 &= 10.08\,. \end{aligned} \tag{2.9}$$

These four values allow to calculate two of the Feigenbaum ratios in Eq.(2.7). The ratios are 0.13, and 0.19. The asymptotic law allows to estimate the accumulation point where chaos sets in. From Eq.(2.7) we derive the estimate

$$\lambda_\infty \approx \frac{\delta\lambda_{\nu+1} - \lambda_\nu}{\delta - 1} \qquad \text{for } \delta = 4.6692 \tag{2.10}$$

and large enough ν. Applying this to our sequence of period doublings in Eq.(2.9), we estimate that λ_∞ is as close as $\lambda_\infty \approx 10.08$.

Related $y_1(t)$-plots of solutions are shown in Figure 5 of Tutorial 1, compare with Figure 5c and Figure 5d (Tutorial 1). Here in Figures 2.13 and 2.14 we show phase plot projections (y_1, y_2) of a periodic orbit of the double period for $\lambda = 10.55$, and of the fourfold period ($\lambda = 10.11$). For smaller values of the parameter with increasing periods the dynamic behavior is “chaotic”, see Figure 2.15.

Another example with period doublings is the voltage-collapse problem WOBexd15.

2.10 Other bifurcations

So far we have introduced three bifurcation mechanisms, namely Hopf bifurcation, turning point (fold bifurcation), and period doubling (flip bifurcation). These three bifurcations are the most important ones for a problem of the type of Eq.(2.2), because they occur most frequently in applications. There are other bifurcation phenomena which we briefly list.

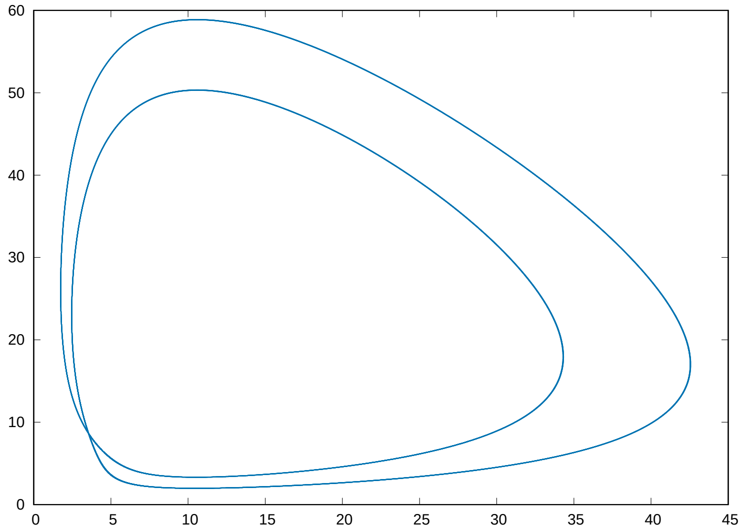

Figure 2.13: Eq.(2.8), $\lambda = 10.55$, (y_1, y_2)-plane, double period

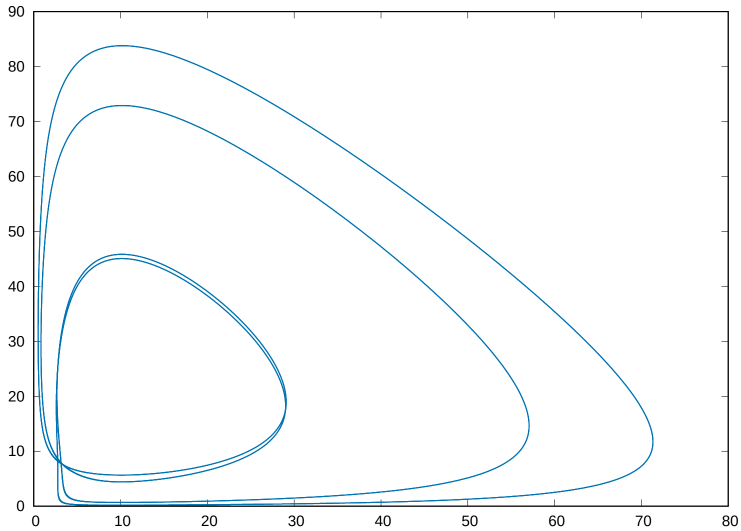

Figure 2.14: Eq.(2.8), $\lambda = 10.11$, (y_1, y_2)-plane, fourfold period

First we return to the pitchfork. The simplest equation with pitchfork is $0 = \lambda y \pm y^3$. The simplest equations exhibiting a certain phenomenon are called *normal forms*. As mentioned above, in case the underlying equation supports a Z_2-symmetry, the pitchfork scenario is also likely to occur. The geometrical analogy of a pitchfork illustration with that of a Hopf bifurcation is no coincidence since the normal form of Hopf bifurcation in polar coordinates ρ, ϑ is

$$\begin{aligned} \dot{\rho} &= \lambda\rho - \rho^3 \\ \dot{\vartheta} &= 1\,. \end{aligned} \tag{2.11}$$

Solutions of this normal form include the stationary state $\rho \equiv 0$, and the periodic state $\rho(t) \equiv \sqrt{\lambda}$. In both cases $\dot{\rho} = 0$ holds, and we have a pitchfork characterization of the amplitude.

In case the equation supports no symmetry, then a pitchfork requires more parameters than just λ. Classifications of related bifurcations of higher *codimension* can be found in [Golubitsky & Schaeffer, 1985]. The higher the codimension, the less likely it is to find a related bifurcation. But bifurcations of higher codimension play a prominent role as organizing centers in parameter space. We shall briefly return to this in the following Section.

Branches of periodic orbits can show more bifurcation phenomena than just period doubling. The multipliers can cross the unit circle of the complex plane at $+1$. Then we encounter,

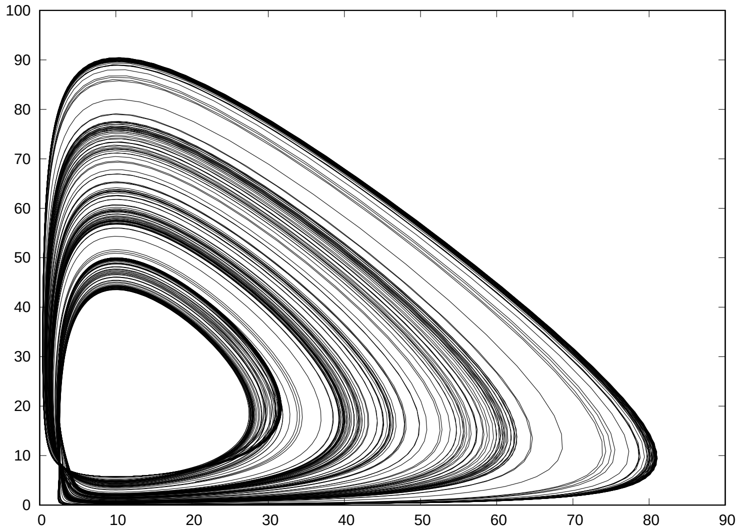

Figure 2.15: Eq.(2.8), $\lambda = 9.99$, (y_1, y_2)-plane, chaos

for example, a turning point, or a pitchfork bifurcation. The turning point of periodic orbits is sometimes called *cyclic fold bifurcation*. When the crossing is with nonzero imaginary part, there is a bifurcation into a torus-like object.

A branch of periodic orbits, born in a Hopf bifurcation, may end in a *homoclinic orbit*. To explain the simplest such scenario imagine in a plane a stationary state of saddle type. This saddle has a pair of entering trajectories and a pair of leaving trajectories. In case the leaving trajectory bends back such that it is identical with the entering trajectory we have a loop with infinite period. This is a homoclinic orbit. Figure 2.16 depicts a periodic stable orbit close to a saddle. Assume this is the situation for $\lambda = \lambda_0 + \epsilon$, and the periodic orbit and the saddle approach each other for $\epsilon \to 0$, and merge for $\epsilon = 0$. Then we encounter a homoclinic orbit for λ_0 and no periodic orbit for $\lambda_0 - \epsilon$.

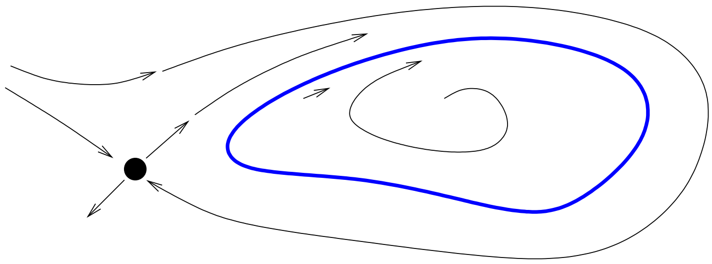

Figure 2.16: Hypothetic phase portrait, with a situation close to a homoclinic orbit: A stable periodic orbit is depicted (blue color), and in the neighborhood a saddle (black dot) with its insets and outsets. Imagine what happens when the saddle and the periodic orbits approach each other. When they merge, we have a homoclinic orbit.

This simplest scenario of a homoclinic orbit illustrates how an unstable stationary state annihilates a periodic orbit. Analogous phenomena are also possible with other unstable states. For example, a collision of an unstable periodic orbit might terminate a chaotic attractor. Generally, unstable states play fundamental roles in organizing dynamical behavior. This situation stresses the importance of calculating unstable states too. An example of the decisive role an unstable state plays in “killing” the operating regime is provided by models of voltage collapse, see WOBexd15.

2.11 Multi-parameter problems

The problems discussed so far depend on one parameter λ. The standard situation in applications is that problems involve several parameters λ, γ, δ, ..., say, m parameters. In freezing $m-1$ parameters to fixed values, and varying only one parameter (say, λ), all the bifurcation phenomena mentioned above may occur. If we unfreeze a second parameter (say, γ), all bifurcation results also depend on γ. In particular, the critical bifurcation values λ_0 vary with γ. In a (λ, γ)-parameter plane the loci of bifurcations are *curves*, the *bifurcation curves*. Specifically, the Hopf bifurcations constitute the *Hopf curves*, and the turning points form the *fold curves*. The points (λ_0, γ_0) where such bifurcation curves meet in the parameter plane are bifurcations of higher singularity.

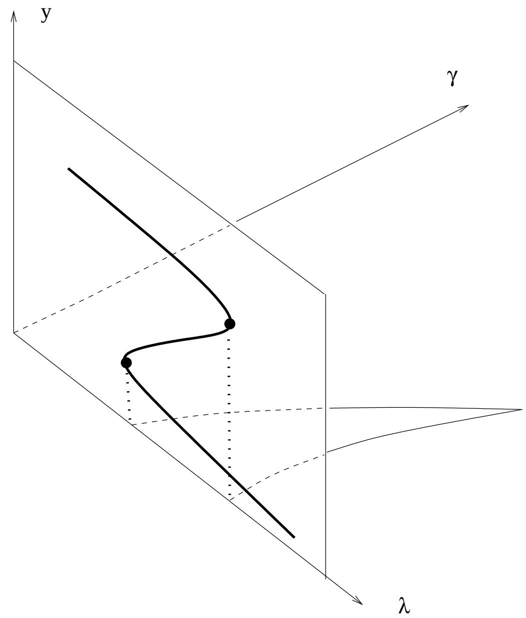

Figure 2.17: Cusp scenario, with two fold curves in a (λ, γ)-plane.

As a simple example, imagine a hysteresis situation as depicted in Figure 2.8. The range of bistability between the values λ_0 of the two turning points may shrink when a second parameter γ is varied, see Figure 2.17. Denote γ_0 the specific value where both $\lambda_0(\gamma)$-curves coincide. Then, on one side of γ_0 (say for $\gamma < \gamma_0$) a bistable situation with jump phenomena exists whereas on the other side no bistability, and no bifurcation of that kind exists. Exactly for $\gamma = \gamma_0$ the bifurcation is a *hysteresis point*, the two adjacent turning points have collapsed into a point of inflection. The value γ_0 is seen as an *organizing center* separating two completely different dynamical situations. This is illustrated by the parameter chart of Figure 2.18. The figure also depicts a jump-free transition from one operation point A in the parameter plane to another (B). A related example is provided by a catalytic reaction (WOBexb1). The knowledge of the bifurcation curves allows to find easily a curve of parameter combinations (λ, γ) that detours and avoids the jumps triggered by turning points (Figure 2.18).

If in addition to λ and γ, a third parameter is considered to be freely variable, then the bifurcation curves in the parameter plane extend to *bifurcation surfaces* in the parameter space. Possible bifurcation scenarios become even more involved. A theory of singularites has been established to analyze related higher-order bifurcations [Golubitsky & Schaeffer, 1985].

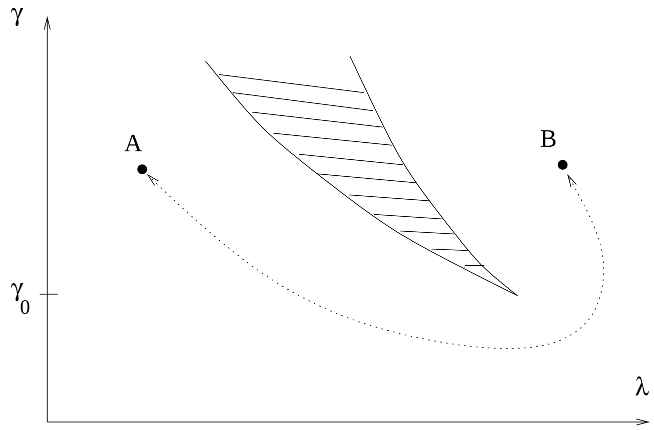

Figure 2.18: Jump-free path (dotted) in a (λ, γ)-parameter plane

2.12 Other problems

The model problem in Eq.(2.2) is a representative of a huge class of applications. But there are other problems equally important, and not covered by Eq.(2.2). For example, many classical oscillation problems are non-autonomous, such as

$$\ddot{u} + f(u, \dot{u}) = \gamma \cos \omega t \tag{2.12}$$

for some function f. The transformation $y_1 := u$, $y_2 := \dot{u}$, $y_3 := t$ leads to a problem of type (2.2), but this transformation may not be always advisable. Another class of problems not immediately of the form in Eq.(2.2) are ODE boundary-value problems

$$\mathbf{y}' = \mathbf{f}(t, \mathbf{y}, \lambda), \quad \mathbf{r}(\mathbf{y}(a), \mathbf{y}(b)) = \mathbf{0}\,. \tag{2.13}$$

Problems of this type describe, for example, *Turing instabilities* that are a mechanism of one-dimensional pattern formation.

The ODE situation discussed so far is a special case of PDEs. PDE models may exhibit ODE bifurcations and many further nonlinear phenomena. Both spatial and temporal phenomena need to be studied. Reaction-diffusion problems of the type

$$\mathbf{y}_t = \mathbf{D}\,\nabla^2\mathbf{y} + \mathbf{f}(\mathbf{y}, \lambda) \tag{2.14}$$

with diffusion matrix $\mathbf{D}$ comprise all ODE settings. For vanishing diffusion ($\mathbf{D} = \mathbf{0}$) the model problem of Eq.(2.2) results. On the other hand, for a stationary situation ($\dot{\mathbf{y}} = \mathbf{0}$, one space variable) the PDE (2.14) reduces to an ODE boundary-value problem of type (12.13). The former case models purely temporal dynamics of the reaction-diffusion problem, whereas the latter case concentrates on purely spatial patterns. In the general case, temporal and spatial phenomena may be interrelated in complicated ways.

2.13 Historical and bibliographical remarks

Early studies of nonlinearity include Euler's buckling problem [1744], and the work of Poincaré [1885]. Classical experimental studies were performed for fluid flow by Bénard [1901], and Taylor [1923]. Analytical investigations are numerous; we mention Liapunov's work on stability [1892], the studies of Andonov and coworkers on "Hopf bifurcation" in the 1930s [1987], Hopf's general theorem [1942], Rayleigh's analysis of convection [1916], and the book by Arnol'd on geometrical methods [1983].

Since the advent of powerful computers and algorithms the field has grown dramatically. The literature is rich, and here is not the space to present a survey. An elementary text book with many examples, algorithms, and practical hints is [Seydel, 2010]. Other texts are oriented more analytically. Early texts include [Guckenheimer & Holmes, 1983], [Golubitsky & Schaeffer, 1985], on Hopf bifurcation [Hassard *et al.*, 1981], and on the chaos-oriented side, [Devaney, 1986].

The applications in this Tutorial are due to the following scientists: Uppal at al [1974] for the continuous stirred tank reactor CSTR Eq.(2.1), Krug & Kuhnert [1985] for the problem from chemistry Eq.(2.4), Pönisch & Schwetlick [1982] for the trigger Eq.(2.5), and Smith et al [1983] for the isothermal reaction Eq.(2.8).

References

Andronov, A.A., Vitt, A.A. & Khaikin, S.E. [1987] *Theory of Oscillators* (Dover Publications, New York).

Arnol'd, V.I. [1983] *Geometrical Methods in the Theory of Ordinary Differential Equations* (Springer, New York).

Bénard, H. [1901] "Les tourbillons cellulaires dans une nappe liquide transportant de la chaleur par convection en regime permanent," *Ann. Chim. Phys.* **7**, Ser. 23, p. 62.

Devaney, R.L. [1986] *An Introduction to Chaotic Dynamical Systems* (Menlo Park, Benjamin).

Euler, L. [1744] "De Curvis Elasticis, Methodus Inveniendi Lineas Curvas Maximi Minimive Proprietate Gaudentes. Additamentum I.," in *Opera Omnia I* Vol.24, 231–297, Zürich 1952.

Golubitsky, M. & Schaeffer, D.G. [1985] *Singularities and Groups in Bifurcation Theory. Vol.1* (Springer, New York).

Guckenheimer, J. & Holmes, Ph. [1983] *Nonlinear Oscillations, Dynamical Systems and Bifurcation of Vector Fields* (Springer, New York).

Hassard, B.D., Kazarinoff, N.D., Wan, Y.-H. [1981] "*Theory and Applications of Hopf Bifurcation* (Cambridge University Press).

Hopf, E. [1942] "Abzweigung einer periodischen Lösung von einer stationären Lösung eines Differentialsystems," (Bericht der Math.-Phys. Klasse der Sächsischen Akademie der Wissenschaften zu Leipzig 94).

Krug, H.-J. & Kuhnert, L. [1985] " Ein oszillierendes Modellsystem mit autokatalytischem Teilschritt," . *Z. Phys. Chemie* **266**, 65–73.

Liapunov, A.M. [1892] *Stability of Motion* (Academic Press, New York, 1966).

Poincaré, H. [1885] "Sur l'équilibre d'une masse fluide animée d'un mouvement de rotation," *Acta Mathematica* **7**, 259–380.

Pönisch, G. & Schwetlick, H. [1982] "Ein lokal überlinear konvergentes Verfahren zur Bestimmung von Rückkehrpunkten implizit definierter Raumkurven," *Numer. Math.* **38**, 455–465.

Lord Rayleigh [1916] "On convection currents in a horizontal layer of fluid, when the higher temperature is on the under side," *Philos. Mag.* **32**, 529–546.

Seydel, R. [2010] *Practical Bifurcation and Stability Analysis. From Equilibrium to Chaos. Third Edition. Springer Interdisciplinary Applied Mathematics, Vol.* **5**. (Springer, New York).

Smith, C.B., Kuszta, B., Lyberatos, G. & Bailey, J.E. [1983] "Period doubling and complex dynamics in an isothermal chemical reaction system," *Chem. Eng. Sci.* **38**, 425–430.

Taylor, G.I. [1923] "Stability of a viscous liquid contained between two rotating cylinders," *Philos. Trans. Roy. Soc. London* **A 223**, 289–343.

Uppal, A., Ray, W.H., Poore, A.B. [1974] "On the dynamic behavior of continuous stirred tank reactors," Chem. Engng. Science **29**, 967–985.